Published in final edited form as:

Cardiovasc Innov Appl. 2016 December 1; 2(1): 31–46. doi:10.15212/CVIA.2016.0052.

Novel SPECT Technologies and Approaches in Cardiac Imaging

Piotr Slomka[*], **Guang-Uei Hung**[†], **Guido Germano**[*], and **Daniel S. Berman**[*]

[*]Departments of Imaging and Medicine, Cedars-Sinai Medical Center, Los Angeles, CA, USA

[†]Department of Nuclear Medicine, Chang Bing Show Chwan Memorial Hospital, Changhua, Taiwan

Abstract

Recent novel approaches in myocardial perfusion single photon emission CT (SPECT) have been facilitated by new dedicated high-efficiency hardware with solid-state detectors and optimized collimators. New protocols include very low-dose (1 mSv) stress-only, two-position imaging to mitigate attenuation artifacts, and simultaneous dual-isotope imaging. Attenuation correction can be performed by specialized low-dose systems or by previously obtained CT coronary calcium scans. Hybrid protocols using CT angiography have been proposed. Image quality improvements have been demonstrated by novel reconstructions and motion correction. Fast SPECT acquisition facilitates dynamic flow and early function measurements. Image processing algorithms have become automated with virtually unsupervised extraction of quantitative imaging variables. This automation facilitates integration with clinical variables derived by machine learning to predict patient outcome or diagnosis. In this review, we describe new imaging protocols made possible by the new hardware developments. We also discuss several novel software approaches for the quantification and interpretation of myocardial perfusion SPECT scans.

Keywords

myocardial perfusion imaging; single photon emission computed tomography; fast myocardial perfusion single photon emission computed tomography; quantification; low dose; stress only

Introduction

This brief review covers the latest technological advances in myocardial perfusion imaging with single photon emission CT (SPECT), referred to hereafter as MPS. We focus on the new types of hardware recently introduced to clinical practice and describe various new imaging protocols made possible by these hardware developments. We also discuss several novel software approaches that have been recently proposed for the quantification and interpretation of nuclear cardiology SPECT scans.

Corresponding Author: Piotr Slomka, Department of Medicine, Cedars-Sinai Medical Center, Los Angeles, CA, USA, piotr.slomka@cshs.org.

Conflict of interest

Cedars-Sinai Medical Center receives royalties for the quantitative assessment of function, perfusion, and viability, a minority portion of which is distributed to some of the authors of this manuscript (PJS, GG, DSB).

New SPECT Systems

Recently, several novel designs of the gantry coupled with new solid-state detectors, which allow increased photon sensitivity in the myocardial region, have been introduced. Novel collimator designs, such as multipinhole and locally focusing collimators configured specifically for cardiac imaging, allow the imaging time and radiation dose to be reduced. The physical space required is also reduced since the dedicated detectors and gantries are significantly smaller than conventional scanners. The new SPECT scanners demonstrate up to an eight-fold increase in photon sensitivity (due to the collimator and imaging geometry) and up to a two-fold increase in image resolution (due to the increased energy resolution of the new crystals).

Because of the new reconstruction techniques using resolution recovery principles, these systems can maintain or improve overall spatial resolution, even if the collimator sensitivity is significantly increased (which typically would reduce image resolution). Increased sensitivity allows much shorter acquisition times, or very low-dose imaging protocols. Shorter imaging times often lead to the additional benefit of reducing patient motion during scans and increasing patient comfort. The improved capabilities of these systems have resulted in the development of various novel imaging strategies, such as fast two-position imaging, flow measurements, early ejection fraction (EF) measurements, and simultaneous dual-isotope imaging as described in this review. More extensive reviews of the new hardware systems can be found elsewhere [1, 2].

Very Low-Dose Imaging Protocols

The list-mode capabilities of the latest SPECT equipment allow realistic simulation of low-dose imaging. Since the list-mode file contains individual count events and timing, it is possible to select only a subset of events (either for a selected time portion of the scan or for the entire duration of the scan). Such an approach allows the creation of a perfect simulation of low-dose imaging (for any dose), without the need to repeat the scan. Various levels of injected activity have been simulated in 79 patients, who were imaged by a high-efficiency scanner for 14 min with 21.7 Å} 5.4 mCi of 99mTc injected at stress [3]. Even with simulated injected activity corresponding to an effective radiation dose of less than 1 mSv, there was no significant difference in the quantitative perfusion parameters (Figure 1). Similarly, functional measurements were not affected. Importantly, however, to preserve the reproducibility between high-count and low-count data, the quantification of the low-dose scans may require specially calibrated normal limits created with low-dose images because of higher variability of the data [4].

The actual comparison of very low-dose imaging with new high-efficiency scanners with standard dose imaging with a conventional scanner was also demonstrated recently in a clinical study by repeated rest scans. The image quality for very low-dose rest scans (with a mean effective dose of 1.15 mSv) was superior to that of conventional SPECT [5]. Recently, the same group demonstrated the results of very low-dose stress-only imaging in 69 patients with a high-efficiency scanner with an average effective radiation dose of 0.99 mSv [6].

Attenuation Correction

The new-generation SPECT scanners are often available in a hybrid configuration with modern high-end 64-slice CT scanners. This setup allows photon attenuation correction and also hybrid imaging for either calcium scoring or coronary CT angiography. Nevertheless, from the clinical workflow standpoint, it may be preferable to operate SPECT and CT scanners separately, for both attenuation correction and coronary anatomic information. Software for interactive and automated alignment of CT scans with MPS scans has been developed [7].

The typical dose from one CT attenuation correction scan (stress or rest) is on the order of 0.3–1.3 mSv [8], which adds substantially to the overall radiation dose, especially for very low dose MPS protocols. To reduce the radiation dose from attenuation correction scans, new designs have been developed for SPECT scanners. An integrated attenuation correction system with an effective dose of 5 μSv has been implemented, in which photons from an X-ray source are detected by solid-state detectors with a fan beam collimator operating in high counting rate mode [9]. Another example of new attenuation correction technology is a flat panel X-ray detector system that provides low-dose (0.12 mSv) CT images that can be used for attenuation correction of SPECT images [10]. Although, not geared exclusively toward nuclear cardiology, this system can be used for low-dose attenuation correction in myocardial perfusion studies. The attenuation scan of the heart can be acquired in a single 60-s rotation with the patient breathing normally. As a result, the attenuation data are averaged over multiple respiratory cycles to match the position of the heart during the SPECT acquisition. Such low-dose attenuation correction systems offer potential advantages (lower cost, fewer SPECT-to-CT registration problems) over full-fledged CT; however, they will not allow CT angiography or accurate calcium scoring.

Two-Position Imaging

New cameras are often not available in SPECT/ CT configurations, or such a setup can be prohibitively expensive, and therefore often do not offer attenuation correction. At the same time, very low-dose cardiac SPECT protocols are being introduced with reduced image counts, challenging the accuracy and the reproducibility of visual reading, especially in the presence of attenuation artifacts. To address this issue, new quantification schemes have been developed in which two sequential scans in two patient positions (supine/ upright or supine/prone – depending on the scanner) are performed, allowing differentiation of true perfusion defects from artifacts, for systems without attenuation correction hardware [11–13]. These two-position protocols add only a few minutes to the time required for standard protocol with most of the new-generation MPS scanners.

Combined analysis of myocardial perfusion images obtained sequentially with the patient in upright and supine positions with the solid-state D-SPECT (Spectrum Dynamics) scanner was evaluated [11]. Quantification was performed jointly from co-registered images obtained in two positions, allowing reduction of false positives, as artifacts tend to shift when the patient position is changed (Figure 2). In comparison with invasive coronary angiography, the combined technique showed a higher area under the receiver operating

characteristic curve than the separate upright or supine analysis. Similar results with two-position imaging applied in the obese population with the D-SPECT scanner were demonstrated [12]. Analogous findings were also demonstrated for the GE NM530c scanner when supine/prone images were used to mitigate attenuation artifacts [13]. Potentially, the two-position approach may also allow the detection of position-related truncation artifacts, which may occur with the limited field-of-view gantry of the new scanners [14].

Motion Correction

Although MPS protocols now use cardiac gating during acquisition for analysis of function, the quantification of perfusion has been most commonly performed on summed (added) image frames from all cardiac gates, without consideration of cardiac motion. It has been suggested that analysis of only the end-diastolic images can improve the detection of coronary disease – particularly in smaller hearts [15]. However, use of end-diastolic images in isolation is not usually suitable for reliable computer quantification at standard or low dose, since they contain only significantly reduced counts. A novel cardiac “motion-frozen” display and quantification technique, using all gated frames and taking cardiac motion into account, has been developed to address this issue [16]. Motion freezing of MPS data is accomplished by detection and subsequent motion tracking of the left ventricular endocardial and epicardial borders, with an established left ventricular myocardial contour extraction algorithm. Subsequently, 3D nonlinear image warping is applied to all phases of the gated data, deforming each image phase to match the position of the end-diastolic phase. The warped images are summed, forming motion-frozen perfusion images. Motion-frozen perfusion quantification has been demonstrated to improve the diagnostic performance in obese patients [17].

Respiratory and patient motion can also have a degrading effect on SPECT images, and several recent studies proposed techniques for mitigating these effects. As image resolution increases with advances in image hardware and software reconstruction, heart motion becomes the dominant degrading factor in MPS. Respiratory motion correction can be applied to conventional dual-head systems by modeling of approximate motion [18]. The feasibility of respiratory motion detection and correction from list-mode data by registration of consecutive short-time image frames has been demonstrated for the new fast MPS systems [19, 20]. Similarly with use of registration of short-time 3D frames from the fast MPS data, patient motion can be corrected. This approach has been demonstrated to reduced false positive perfusion defects [21]. Dual respiratory/cardiac-gated MPS imaging has been demonstrated in phantoms, and in patients showing progressive improvement of the myocardium to blood pool contrast when respiratory and cardiac dual gating was applied [22]. Respiratory gating of fast MPS has been shown to affect functional cardiac parameters (wall motion and volumes) [23]. A dual motion-frozen approach for respiratory and cardiac motion correction for cardiac SPECT systems has also been demonstrated [24].

Recent Developments in Automation of Processing

When MPS images are read by clinicians, usually manual scoring of perfusion is performed, often with the aid of computer scoring. However, manual scoring of the stress and rest

perfusion scans in nuclear cardiology is associated with significant variability. Therefore, automated quantification of MPS images has been developed by several groups, and these methods are increasingly used in clinical practice [25–28]. The overall accuracy of these quantitative methods is similar to that of experienced clinicians for studies with or without attenuation correction as recently shown in a large study [29]. These quantification methods require accurate computer segmentation of the myocardium, which may be challenging because of potential perfusion defects, activity outside the myocardium, and image noise. Therefore, currently, supervision by an operator is still required to verify myocardial segmentation. Typically, this is performed by the imaging technologist, before the scan interpretation by the physician.

Several methods for improved automation of MPS scan quantification have been proposed recently. For example, a new method that checks automatically derived myocardial contours for potential segmentation failures has been shown to reduce further the level of human supervision required [30]. This algorithm derives quality control scores to define the probability of the segmentation failure. Two scores are derived: the “shape flag” to detect mask failure cases, and the “valve-plane flag” to detect mitral valve plane mispositioning. This approach has been compared with expert technologists, and was found to be virtually equivalent to expert readers in the identification of failures.

A related novel development is the so-called group or same patient processing method where multiple SPECT scans from the same patient are processed jointly to improve contour detection by avoiding interstudy inconsistencies. These new algorithms can lead to almost full automation of the image analysis steps, with a contour failure rate generally below 1% [31]. The repeatability of the quantitative parameters obtained by grouped analysis has been shown to be approximately half of that obtained by standard quantification [32]. Such methods combined with quality control flags for automatically derived left ventricular contours would allow readers to target manual adjustment only to those few remaining studies flagged by the algorithm for potential errors [30]. Further refinement of automated contours has been proposed, using machine learning methods for fully automated mitral valve placement on cardiac SPECT studies [33], since the precise position of the valve plane is important for accurate quantification of perfusion on the polar maps. In that study, automated positioning of the valve plane on MPS images obtained with the latest generation SPECT scanners had less variability than the variability in positioning between two experienced observers and resulted in similar anatomical position and equivalent diagnostic accuracy as verified by external CT angiography and invasive angiography data (Figure 3). These tools, with further refinement, will ultimately allow fully unsupervised automated perfusion scoring and quantification of myocardial function without compromising accuracy.

Quantification of Ischemic Change

A particularly useful application of quantitative analysis is the estimation of subtle changes in ischemic burden during longitudinal follow-up of the same patient. Image change analysis can provide a reliable objective measure of a patient’s response to therapy. While this can also be performed with visual assessment, small, but clinically important improvements can be under interpreted because of the subjective scoring of different readers. The most

common approach using quantitative analysis is to report the difference in the overall quantitative parameter between repeated scans such as total perfusion deficit – and this has shown good reproducibility and repeatability [34, 35].

The newer automated software can further refine longitudinal follow-up by analyzing serial stress/ rest studies together in pairs, thereby eliminating errors associated with multiple comparisons to normal limits and variations in contour placements [36, 37]. This approach also has the advantage that it does not require normal limits.

Simultaneous Dual-Isotope Imaging

The superior energy resolution of the new solidstate cadmium zinc telluride (CZT) detectors can allow better separation of photons from different isotopes and improved cross-talk correction [38]. In addition, stationary detector system design eliminates the projection consistencies that would further confound the simultaneous dual-isotope imaging. The increased sensitivity of the new scanners is also a key factor in facilitating the imaging of multiple isotopes simultaneously. One possible clinical application is to simultaneously image 99mTc and 201Tl in a combined rest/stress protocol as originally proposed for standard cameras [39], but this has not been implemented clinically before because of technical difficulties.

A proof of concept of simultaneous dual-isotopeimaging with a multipinhole system was recently demonstrated [40]. Simultaneous dual-isotope imaging of 148 MBq of 201Tl (stress) and 222 MBq of 99mTc (rest) was performed immediately after completion of exercise by a three-detector 18-pinhole system during a single 20-min imaging session. The feasibility of simultaneous dual-isotope application was demonstrated with a CZT fast MPS system in 24 patients with simultaneous dual-isotope imaging [41]. Eighty megabecquerels (MBq) of 201Tl (rest) and 250 MBq of technetium (99mTc) sestamibi (stress) were injected during adenosine infusion. Images were acquired for a 15-min list-mode simultaneous dual-radionuclide (rest/stress) gated acquisition with a spillover and scatter correction method, specifically designed for the solid-state camera. Diagnostic performance and image quality, comparable to those of conventional SPECT with a separate rest 201Tl acquisition with a CZT camera, have been demonstrated [38].

Other novel applications of simultaneous dual-isotope imaging with the new CZT cameras have been demonstrated. The feasibility of simultaneous imaging of inflammation with 111 In-labeled white cells and myocardial perfusion with technetium (99mTc) sestamibi was demonstrated in the phantom and in 34 patients [42]. Simultaneous imaging of fatty metabolism with 123I-β-methyliodophenylpentadecanoic acid and perfusion with technetium (99mTc) sestamibi has been shown in 30 patients [43]. An 123I-metaio dobenzylguanidine/201Tl imaging protocol has been proposed for evaluation of trigger zones after revascularization [44].

Stress-Only Imaging

Current MPS protocols require a patient to spend 3–4 h in the laboratory for two separate SPECT scans and are associated with substantial radiation exposure [45]. Stress-only MPS

could limit radiation exposure (up to 60% [46]), increase patient throughput, and lower the cost by eliminating additional imaging time and radiopharmaceutical dose. The total protocol time, including the stress test, can be shortened to 30–45 min. Stress-only protocols with new fast MPS hardware can further reduce imaging time and radiation dose. The prognosis of a normal stress-only study has been confirmed in more than 8,000 patients, and appears to be no different from the prognosis of the standard rest/stress study [46]. In addition to the reduction of the patient radiation dose, the stress-only protocol also allows a significant reduction of the dose to the staff performing the scan [47].

Nevertheless, stress-only imaging is cumbersome to implement, as it requires physician review of images and clinical data (immediately after the stress scan) to determine whether the scan is normal before the rest scan is canceled. To be certain about the normal result in equivocal cases, the physician may need to consider images obtained in two different positions [48] or with attenuation correction [49, 50]. Thus the main barrier to the wide clinical acceptance of the stress-only protocols is the need for the physician to immediately and comprehensively review complex images and clinical data. Efforts have been undertaken to develop clinical scoring models to select patients for stress-only MPS scans [51]. It is likely that the automated image quantification will be of great importance in utilizing such models, as it would allow rapid selection of patients, for which the rest scan could be canceled.

Hybrid CT Angiography–SPECT

One novel SPECT development is the use of hybrid SPECT/CT technology available on the new scanners [52]. Recent advances in CT angiography allow routine dose reduction in the prospective mode to the sub-millisievert range [53]. These new developments allow combined CT and MPS with acceptable radiation burden. The feasibility of a stress-only MPS/CT angiography protocol has been demonstrated in 100 patients and a 1-day adenosine stress/rest protocol with low-dose CT attenuation correction combined with CT angiography obtained with a separate 64-slice CT scanner [54]. The total patient time scheduled of the hybrid CT angiography/stress-MPS examination protocol was 130 min, which is shorter than current 1-day stress/rest MPS protocols. The principal drawback of this approach is that clinicians usually do not know ahead of time which patients will require both coronary and MPS studies; therefore selective and sequential application of imaging modalities may prove to be the optimal approach. Novel techniques that use co-registered prior CT angiography data for the improved quantification of MPS data have been proposed [55] (Figure 4).

Similarly, the additive value of a calcium scan to an MPS scan has been demonstrated by several studies [56, 57]. The new SPECT/CT equipment allows acquisition of a CT calcium scan and the use of the calcium scan for attenuation correction as noted earlier. It has been demonstrated that attenuation correction can be performed with a stand-alone CT calcium scan (which is obtained with cardiac gating) [58], allowing additionally the incorporation of calcium scan results in the overall diagnosis. Even standard attenuation maps could be considered for calcium scoring and diagnostic integration with MPS [59]. It has also been reported that if standard attenuation maps are visually evaluated for the presence of calcium,

they can improve both the prognostic and the diagnostic accuracy of MPS [60, 61]. It has been suggested that calcium scanning should become a routine part of MPS [56].

Dynamic Flow with SPECT

Absolute myocardial blood flow (MBF) and myocardial flow reserve (MFR) are physiological variables related to heart disease. The variables have been shown to provide clinically useful information beyond that provided by MPS assessment of relative perfusion defects. Potentially, absolute measurements can identify multivessel coronary artery disease and predict the extent of disease more accurately than relative perfusion quantification or visual interpretation of MPS scans, which are the clinical standards today [62, 63]. MFR has also demonstrated value as a marker for adverse cardiac events, providing additional risk stratification beyond that provided by assessment of relative perfusion defects alone [64–67]. To date, these flow measurements have been obtained with PET, but with a new generation of SPECT equipment, several recent reports have demonstrate the potential of obtaining these measurements with SPECT.

Human dynamic SPECT flow studies have been demonstrated with a high-efficiency dedicated SPECT system, with factor analysis and a two-compartment model used for quantification [68]. The clinical feasibility of such an approach was demonstrated in 95 patients. The data were reconstructed to 3-s frames, resulting in 60–70 frames for each stress and rest study. Images of the initial frames and the quantification obtained in such a study are shown in Figure 5. This study did not use attenuation correction. The authors demonstrated that MFR derived from such studies was higher in patients with normal scans (as established by standard relative quantification) and that lower MFR (both regional and global) was associated with stress perfusion defect on static imaging, age, and smoking. MFR also showed a stepwise reduction related to the severity of the obstructive disease in a subset of 20 patients, for whom invasive coronary angiography images were available.

Flow measurements for technetium (99mTc) sestamibi, technetium (99mTc) tetrofosmin, and 201Tl have been demonstrated with the latest-generation high-sensitivity SPECT equipment in a study in 19 pigs [70]. The SPECT images were acquired during the tracer injection in list mode and reconstructed as nine 10-s, six15-s, and four 2-min frames (total time 11 min). One-tissue compartmental modeling, similar to that used in 82Rb PET, and extraction correction based on the fit of the microsphere data, was utilized. Good correlations of MBF ($r = 0.75–0.90$) compared with invasive microsphere measurements for all tracers studied and somewhat worse correlations of MFR were shown. The authors also showed recently in subsequent animal studies that low-dose SPECT flow measurements are feasible with such a solid-state camera with doses as low as one-quarter of the standard dose for 99mTc and a half dose for 201Tl [71]. Recently, human validation studies have been performed comparing fast SPECT and PET flow directly. In a study of 28 consecutive patients undergoing fast MPS with attenuation correction and 13N-ammonia, K1 and MFR were computed for SPECT and PET but without use of any extraction fraction correction for technetium (99mTc) tetrofosmin [72]. The authors demonstrated technical feasibility but found that the hyperemic flow values (as expected), and consequently MFR, were lower than

the values obtained by PET. Nevertheless, they concluded that such flow measurements can still have potential diagnostic value.

SPECT flow measurements have also been demonstrated to be feasible with conventional SPECT equipment. Twenty-one patients with suspected and known disease and correlating invasive angiography findings were studied with a conventional dual-head SPECT/CT camera, using multiple backand- forth gantry rotations consisting of 10Å~10 s, 5Å~20 s, 4Å~60 s, and 1Å~280 s for a duration of 12 min [73], and a standard rest/stress technetium (99mTc) sestamibi dosing regimen. The reconstruction was performed with attenuation and scatter correction and resolution recovery. Flow measurements were computed by standard one-compartment modeling using the extraction fraction/flow relationship established previously by Leppo and Meerdink [74] in animal models. The result was a significantly higher area under the operating curve with MFR and stress MBF than with the traditional visual interpretation of perfusion images for the detection of 50% or higher stenosis. The authors also demonstrated that quantitative flow results are potentially less accurate if these physical corrections are not performed. In another recent study from the same group, 28 patients were studied with conventional SPECT/ CT, and the flow-dependent extraction fraction relationship was determined by the fitting of the SPECT quantification results to the 13N-ammonia results [75]. With this approach, very good correlations were obtained for global and regional MBF and MFR by technetium (99mTc) sestamibi SPECT and 13N-ammonia PET (R2=0.71–0.92). Technetium (99mTc) tetrofosmin SPECT MBF and MFR measurements have also been reported in 16 patients with use of standard slow rotation dual-head camera equipment and a special 4D reconstruction approach, which allowed derivation of dynamic information from a limited projection dataset [76]. Direct comparison with 13N-ammonia PET showed good MBF correlation but only moderate MFR correlation.

Although quantitative flow analysis with SPECT has been demonstrated as feasible in some recent studies, several obstacles still need to be overcome. The low count data remain a challenge for conventional MPS. Fast MPS may solve this problem, but it is not yet widely used. In particular, CT-based attenuation correction is not commonly available for SPECT systems and especially is not typically available for fast MPS systems. Further, extensive validation is needed, particularly by direct comparison with a gold standard, such as PET measurements with 13N-ammonia or 15O. The potential of stress-only peak flow MBF measurements with technetium (99mTc) sestamibi should be explored. Finally, clinical algorithms integrating relative perfusion findings with absolute flow quantification, as well as with other clinical and imaging data, should be firmly established to optimally guide patient treatment and demonstrate the added value of this new tool.

Early EF Imaging

Since the measurement of MBF and MFR by SPECT requires early acquisition immediately after the injection, and not 15–40 min after the injection (as usually performed in MPS), a possible additional measurement that could be made during such early images is measurement of EF reserve (an increase or drop in EF during stress). Fast MPS hardware can facilitate such protocols. High EF reserve was shown to have excellent negative predictive value in exclusion of severe coronary artery disease by dipyridamole stress 82Rb

PET [77]. Recently the feasibility of early EF measurements has been demonstrated in 50 patients scanned with a dedicated solid-state SPECT scanner [78]. Significantly lower mean EF reserve was obtained in the fifth and the ninth minute after regadenoson bolus in patients with significant ischemia versus patients without significant ischemia. In the future, it may be feasible to obtain measurements of EF reserve and MFR from the same early rest/stress SPECT scans.

Machine Learning for Improved Diagnosis and Prognosis

Machine learning is a field of computer science that uses mathematical algorithms to identify patterns in data, building computational models, which allow data-driven predictions or decisions. MPS offers an interesting application for machine learning because it provides multiple imaging and clinical variables that could be combined to improve the diagnosis or the accuracy of the prognosis. For example, automatically derived functional cardiac parameters and perfusion parameters both carry some diagnostic information, and physicians try to combine this information in their minds when arriving at the final diagnosis. A recent study showed that the overall diagnostic accuracy of conventional cardiac SPECT could be improved by combining perfusion and functional parameters with a machine learning algorithm [79].

The final clinical diagnosis after MPS, however, usually includes more information than is available from the images. During MPS reporting, clinicians typically also consider information such as patient, age, history, and other clinical findings, which together form a pretest risk profile. Several recent SPECT studies demonstrated that it is feasible to combine such clinical information with quantitative image information and derive enhanced composite diagnostic or prognostic scores to predict disease or patient outcome.

In 1188 patients who underwent cardiac SPECT scans, an ensemble machine learning method (LogitBoost) was compared with standard quantitative perfusion assessment from images (total perfusion deficit) and visual scores by experienced physicians using clinical information. When clinical information was provided to the machine learning algorithm in addition to the imaging features, machine learning achieved a higher area under the receiver operating curve (0.94 Å) 0.01) than did total perfusion deficit (0.88 Å) 0.01) or two visual readers (0.89, 0.85) for the detection of disease (Figure 6) [80]. Machine learning application has also been shown for prediction of revascularization after SPECT. The prediction of revascularization by machine learning was compared with standalone measures of perfusion and visual analysis by two experienced readers using all imaging, quantitative, and clinical data. The area under the receiver operating curve for machine learning was similar to that for experienced readers and automated measure of perfusion [81].

Summary

Recent novel approaches in MPS have been facilitated by the availability of dedicated high-efficiency hardware with solid-state detectors and optimized collimators. New protocols include very low-dose (1 mSv) stress-only imaging, two-position imaging to mitigate attenuation artifacts, and simultaneous dual-isotope imaging (leveraging increased energy

resolution). Attenuation correction can be performed by specialized very low-dose systems or even by previously obtained CT coronary calcium scans. Hybrid imaging protocols using CT angiography have been proposed. Fast SPECT acquisition also facilitates dynamic flow and early function measurements. New reconstruction techniques increase image resolution. Further image quality improvements have been demonstrated by novel methods for cardiac, respiratory, and patient motion corrections. Image processing algorithms have recently become much more automated, with virtually unsupervised extraction of quantitative variables from the images. This automation facilitates integration with clinical variables derived by machine learning to predict patient outcome or diagnosis.

Acknowledgments

This research was supported in part by grant R01HL089765 from the National Heart, Lung, and Blood Institute/ National nstitutes of Health (NHLBI/NIH). Its contents are solely the responsibility of the authors and do not necessarily represent the official views of the NHLBI/NIH. We thank Joanna Liang for proofreading the paper.

References

1. Slomka PJ, Pan T, Berman DS, Germano G. Advances in SPECT and PET Hardware. Prog Cardiovasc Dis. 2015; 57(6):566–78. [PubMed: 25721706]
2. Slomka PJ, Berman DS, Germano G. New cardiac cameras: single-photon emission CT and PET. Semin Nucl Med. 2014; 44(4):232–51. [PubMed: 24948149]
3. Nakazato R, Berman DS, Hayes SW, et al. Myocardial Perfusion Imaging with a Solid-State Camera: Simulation of a Very Low Dose Imaging Protocol. J Nucl Med. 2013; 54(3):373–9. [PubMed: 23321457]
4. Slomka PJ, Rubeaux M, Germano G. Quantification with normal limits: New cameras and low-dose imaging. J Nucl Cardiol. 2016 Jun 14. [Epub ahead of print].
5. Einstein AJ, Blankstein R, Andrews H, et al. Comparison of image quality, myocardial perfusion, and left ventricular function between standard imaging and single-injection ultra-low-dose imaging using a high-efficiency SPECT camera: the MILLISIEVERT study. J Nucl Med. 2014; 55(9):1430–7. [PubMed: 24982439]
6. Einstein AJ, Johnson LL, DeLuca AJ, et al. Radiation dose and prognosis of ultra-low-dose stress-first myocardial perfusion SPECT in patients with chest pain using a high-efficiency camera. J Nucl Med. 2015; 56(4):545–51. [PubMed: 25745089]
7. Slomka PJ, Diaz-Zamudio M, Dey D, et al. Automatic registration of misaligned CT attenuation correction maps in Rb-82 PET/CT improves detection of angiographically significant coronary artery disease. J Nucl Cardiol. 2015; 22(6):1285–95. [PubMed: 25698471]
8. Einstein AJ, Johnson LL, Bokhari S, et al. Agreement of Visual Estimation of Coronary Artery Calcium From Low-Dose CT Attenuation Correction Scans in Hybrid PET/CT and SPECT/CT With Standard Agatston Score. Journal of the American College of Cardiology. 2010; 56(23):1914–21. [PubMed: 21109114]
9. Conwell R, Babla H, Gurley M, et al. Phantom evaluation of a cardiac SPECT/VCT system that uses a common set of solid-state detectors for both emission and transmission scans. Journal of Nuclear Cardiology. 2010; 17(3):459–69. [PubMed: 20169476]
10. Franc BL, Myers R, Pounds TR, et al. Clinical utility of SPECT-(low-dose)CT versus SPECT alone in patients presenting for bone scintigraphy. Clin Nucl Med. 2012; 37(1):26–34. [PubMed: 22157024]
11. Nakazato R, Tamarappoo BK, Kang X, et al. Quantitative upright-supine high-speed SPECT myocardial perfusion imaging for detection of coronary artery disease: correlation with invasive coronary angiography. J Nucl Med. 2010; 51(11):1724–31. [PubMed: 20956478]
12. Nakazato R, Slomka PJ, Fish M, et al. Quantitative high-efficiency cadmium-zinc-telluride SPECT with dedicated parallel-hole collimation system in obese patients: results of a multi-center study. J Nucl Cardiol. 2015; 22(2):266–75. [PubMed: 25388380]

13. Duvall WL, Slomka PJ, Gerlach JR, et al. High-efficiency SPECT MPI: comparison of automated quantification, visual interpretation, and coronary angiography. J Nucl Cardiol. 2013; 20(5):763–73. [PubMed: 23737160]
14. Fiechter M, Gebhard C, Fuchs TA, et al. Cadmium-zinc-telluride myocardial perfusion imaging in obese patients. Journal of Nuclear Medicine. 2012; 53(9):1401–6. [PubMed: 22870823]
15. Taillefer R, DePuey EG, Udelson JE, Beller GA, Benjamin C, Gagnon A. Comparison between the end-diastolic images and the summed images of gated 99mTc-sestamibi SPECT perfusion study in detection of coronary artery disease in women. J Nucl Cardiol. 1999; 6(2):169–76. [PubMed: 10327101]
16. Slomka PJ, Nishina H, Berman DS, et al. "Motion-frozen" display and quantification of myocardial perfusion. J Nucl Med. 2004; 45(7):1128–34. [PubMed: 15235058]
17. Suzuki Y, Slomka P, Wolak A, et al. 26.02--10:40 a.m. : "Motion-frozen" Myocardial Perfusion SPECT Improves Detection of CAD in Obese Patients. Journal of Nuclear Cardiology. 2007; 14(4):S124–528.
18. Qi W, Yang Y, Wernick MN, Pretorius PH, King MA. Limited-angle effect compensation for respiratory binned cardiac SPECT. Med Phys. 2016; 43(1):443. [PubMed: 26745937]
19. Daou D, Sabbah R, Coaguila C, Boulahdour H. Feasibility of data-driven cardiac respiratory motion correction of myocardial perfusion CZT SPECT: A pilot study. J Nucl Cardiol. 2016 May 11. [Epub ahead of print].
20. Daou D, Sabbah R, Coaguila C, Boulahdour H. Applicability of data-driven respiratory motion correction to CZT SPECT myocardial perfusion imaging in the clinical setting: The birth of an old wish. J Nucl Cardiol. 2016 Aug 18. [Epub ahead of print].
21. Kennedy JA, William Strauss H. Motion detection and amelioration in a dedicated cardiac solid-state CZT SPECT device. Medical & biological engineering & computing. 2016 Jul 14. [Epub ahead of print].
22. Chan C, Harris M, Le M, et al. End-expiration respiratory gating for a high-resolution stationary cardiac SPECT system. Phys Med Biol. 2014; 59(20):6267–87. [PubMed: 25256033]
23. Buechel RR, Husmann L, Pazhenkottil AP, et al. Myocardial perfusion imaging with real-time respiratory triggering: impact of inspiration breath-hold on left ventricular functional parameters. J Nucl Cardiol. 2010; 17(5):848–52. [PubMed: 20414755]
24. Kovalski G, Keidar Z, Frenkel A, Sachs J, Attia S, Azhari H. Dual "motion-frozen heart" combining respiration and contraction compensation in clinical myocardial perfusion SPECT imaging. J Nucl Cardiol. 2009; 16(3):396–404. [PubMed: 19159994]
25. Germano G, Kavanagh PB, Slomka PJ, Van Kriekinge SD, Pollard G, Berman DS. Quantitation in gated perfusion SPECT imaging: The Cedars-Sinai approach. Journal of Nuclear Cardiology. 2007; 14(4):433–54. [PubMed: 17679052]
26. Garcia EV, Faber TL, Cooke CD, Folks RD, Chen J, Santana C. The increasing role of quantification in clinical nuclear cardiology: the Emory approach. J Nucl Cardiol. 2007; 14(4): 420–32. [PubMed: 17679051]
27. Ficaro EP, Lee BC, Kritzman JN, Corbett JR. Corridor4DM: the Michigan method for quantitative nuclear cardiology. J Nucl Cardiol. 2007; 14(4):455–65. [PubMed: 17679053]
28. Liu YH. Quantification of nuclear cardiac images: the Yale approach. J Nucl Cardiol. 2007; 14(4): 483–91. [PubMed: 17679055]
29. Arsanjani R, Xu Y, Hayes SW, et al. Comparison of fully automated computer analysis and visual scoring for detection of coronary artery disease from myocardial perfusion SPECT in a large population. J Nucl Med. 2013; 54(2):221–8. [PubMed: 23315665]
30. Xu Y, Kavanagh P, Fish M, et al. Automated quality control for segmentation of myocardial perfusion SPECT. J Nucl Med. 2009; 50(9):1418–26. [PubMed: 19690019]
31. Germano G, Kavanagh P, Fish M, et al. "Same-Patient Processing" for multiple cardiac SPECT studies. 1. Improving LV segmentation accuracy. J Nucl Cardiol 2016. 2016; 23(6):1435–41.
32. Germano G, Kavanagh PB, Ruddy TD, et al. "Same-patient processing" for multiple cardiac SPECT studies. 2. Improving quantification repeatability. J Nucl Cardiol. 2016; 23(6):1442–53. [PubMed: 27743297]

33. Betancur J, Rubeaux M, Fuchs T, et al. Automatic Valve Plane Localization in Myocardial Perfusion SPECT/CT by Machine Learning: Anatomical and Clinical Validation. J Nucl Med. 2016 Nov 3. [Epub ahead of print].
34. Xu Y, Hayes S, Ali I, et al. Automatic and visual reproducibility of perfusion and function measures for myocardial perfusion SPECT. Journal of Nuclear Cardiology. 2010; 17(6):1050–7. [PubMed: 20963537]
35. Berman DS, Kang X, Gransar H, et al. Quantitative assessment of myocardial perfusion abnormality on SPECT myocardial perfusion imaging is more reproducible than expert visual analysis. Journal of Nuclear Cardiology. 2009; 16(1):45–53. [PubMed: 19152128]
36. Slomka PJ, Nishina H, Berman DS, et al. Automatic quantification of myocardial perfusion stress-rest change: a new measure of ischemia. J Nucl Med. 2004; 45(2):183–91. [PubMed: 14960634]
37. Prasad M, Slomka PJ, Fish M, et al. Improved quantification and normal limits for myocardial perfusion stress-rest change. J Nucl Med. 2010; 51(2):204–9. [PubMed: 20124046]
38. Kacperski, K., Erlandsson, K., Ben-Haim, S., Van Gramberg, D., Hutton, BF. Iterative deconvolution of simultaneous dual radionuclide projections for CdZnTe based cardiac SPECT. IEEE Nuclear Science Symposium Conference Record, 2008 NSS'08; 2008. p. 5260-3.
39. Kiat H, Germano G, Friedman J, et al. Comparative feasibility of separate or simultaneous rest thallium-201/stress technetium-99m-sestamibi dual-isotope myocardial perfusion SPECT. Journal of Nuclear Medicine. 1994; 35(4):542. [PubMed: 8151372]
40. Steele PP, Kirch DL, Koss JE. Comparison of Simultaneous Dual-Isotope Multipinhole SPECT with Rotational SPECT in a Group of Patients with Coronary Artery Disease. Journal of Nuclear Medicine. 2008; 49(7):1080. [PubMed: 18552149]
41. Ben-Haim S, Kacperski K, Hain S, et al. Simultaneous dual-radionuclide myocardial perfusion imaging with a solid-state dedicated cardiac camera. Eur J Nucl Med Mol Imaging. 2010; 37(9): 1710–21. [PubMed: 20383705]
42. Caobelli F, Wollenweber T, Bavendiek U, et al. Simultaneous dual-isotope solid-state detector SPECT for improved tracking of white blood cells in suspected endocarditis. Eur Heart J. 2016 Jul 28. [Epub ahead of print].
43. Ko T, Utanohara Y, Suzuki Y, et al. A preliminary feasibility study of simultaneous dual-isotope imaging with a solid-state dedicated cardiac camera for evaluating myocardial perfusion and fatty acid metabolism. Heart and vessels. 2016; 31(1):38–45. [PubMed: 25217037]
44. D'Estanque E, Hedon C, Lattuca B, et al. Optimization of a simultaneous dual-isotope 201Tl/123I-MIBG myocardial SPECT imaging protocol with a CZT camera for trigger zone assessment after myocardial infarction for routine clinical settings: Are delayed acquisition and scatter correction necessary? J Nucl Cardiol. 2016 May 25. [Epub ahead of print].
45. Bourque JM, Beller GA. Stress myocardial perfusion imaging for assessing prognosis: an update. JACC: Cardiovascular Imaging. 2011; 4(12):1305–19. [PubMed: 22172788]
46. Chang SM, Nabi F, Xu J, Raza U, Mahmarian JJ. Normal stress-only versus standard stress/rest myocardial perfusion imaging: similar patient mortality with reduced radiation exposure. J Am Coll Cardiol. 2010; 55(3):221–30. [PubMed: 19913381]
47. Duvall WL, Guma KA, Kamen J, et al. Reduction in occupational and patient radiation exposure from myocardial perfusion imaging: impact of stress-only imaging and high-efficiency SPECT camera technology. J Nucl Med. 2013; 54(8):1251–7. [PubMed: 23723432]
48. Des Prez RD, Dahlberg ST, Einstein AJ, Grossman GB, Henzlova MJ, Mahenthiran J, Vashist A. ASNC clinical update: Stress-only myocardial perfusion imaging. J Nucl Cardiol. 2009; 16:329–31.
49. Bateman TM, Heller GV, McGhie AI, et al. Multicenter investigation comparing a highly efficient half-time stress-only attenuation correction approach against standard rest-stress Tc-99m SPECT imaging. Journal of Nuclear Cardiology. 2009; 16(5):726–35. [PubMed: 19548048]
50. Gibson PB, Demus D, Noto R, Hudson W, Johnson LL. Low event rate for stress-only perfusion imaging in patients evaluated for chest pain. Journal of the American College of Cardiology. 2002; 39(6):999–1004. [PubMed: 11897442]

51. Duvall WL, Baber U, Levine EJ, Croft LB, Henzlova MJ. A model for the prediction of a successful stress-first Tc-99m SPECT MPI. J Nucl Cardiol. 2012; 19(6):1124–34. [PubMed: 23076554]
52. Slomka PJ, Berman DS, Germano G. Applications and software techniques for integrated cardiac multimodality imaging. Expert review of cardiovascular therapy. 2008; 6(1):27–41. [PubMed: 18095905]
53. Stehli J, Fuchs TA, Bull S, et al. Accuracy of coronary CT angiography using a submillisievert fraction of radiation exposure: comparison with invasive coronary angiography. J Am Coll Cardiol. 2014; 64(8):772–80. [PubMed: 25145520]
54. Husmann L, Herzog BA, Gaemperli O, et al. Diagnostic accuracy of computed tomography coronary angiography and evaluation of stress-only single-photon emission computed tomography/computed tomography hybrid imaging: comparison of prospective electrocardiogram-triggering vs. retrospective gating. European Heart Journal. 2009; 30(5):600. [PubMed: 19106197]
55. Slomka PJ, Cheng VY, Dey D, et al. Quantitative analysis of myocardial perfusion SPECT anatomically guided by coregistered 64-slice coronary CT angiography. J Nucl Med. 2009; 50(10): 1621–30. [PubMed: 19759104]
56. Rozanski A, Slomka P, DSB. Extending the Use of Coronary Calcium Scanning to Clinical Rather Than Just Screening Populations: Ready for Prime Time? Circ Cardiovasc Imaging. 2016; 9(5)
57. Brodov Y, Gransar H, Dey D, et al. Combined Quantitative Assessment of Myocardial Perfusion and Coronary Artery Calcium Score by Hybrid 82Rb PET/CT Improves Detection of Coronary Artery Disease. J Nucl Med. 2015; 56(9):1345–50. [PubMed: 26159582]
58. Schepis T, Gaemperli O, Koepfli P, et al. Use of coronary calcium score scans from stand-alone multislice computed tomography for attenuation correction of myocardial perfusion SPECT. European journal of nuclear medicine and molecular imaging. 2007; 34(1):11–9. [PubMed: 16896667]
59. Einstein AJ, Johnson LL, Bokhari S, et al. Agreement of visual estimation of coronary artery calcium from low-dose CT attenuation correction scans in hybrid PET/CT and SPECT/CT with standard Agatston score. J Am Coll Cardiol. 2010; 56(23):1914–21. [PubMed: 21109114]
60. Patchett ND, Pawar S, Miller EJ. Visual identification of coronary calcifications on attenuation correction CT improves diagnostic accuracy of SPECT/CT myocardial perfusion imaging. J Nucl Cardiol. 2016 Feb 5. [Epub ahead of print].
61. Engbers EM, Timmer JR, Mouden M, et al. Visual estimation of coronary calcium on computed tomography for attenuation correction. J Cardiovasc Comput Tomogr. 2016; 10(4):327–9. [PubMed: 27089854]
62. Hajjiri MM, Leavitt MB, Zheng H, Spooner AE, Fischman AJ, Gewirtz H. Comparison of positron emission tomography measurement of adenosine-stimulated absolute myocardial blood flow versus relative myocardial tracer content for physiological assessment of coronary artery stenosis severity and location. JACC Cardiovasc Imaging. 2009; 2(6):751–8. [PubMed: 19520347]
63. Fiechter M, Ghadri JR, Gebhard C, et al. Diagnostic value of 13N-ammonia myocardial perfusion PET: added value of myocardial flow reserve. J Nucl Med. 2012; 53(8):1230–4. [PubMed: 22776752]
64. Herzog BA, Husmann L, Valenta I, et al. Long-term prognostic value of 13N-ammonia myocardial perfusion positron emission tomography added value of coronary flow reserve. J Am Coll Cardiol. 2009; 54(2):150–6. [PubMed: 19573732]
65. Fukushima K, Javadi MS, Higuchi T, et al. Prediction of short-term cardiovascular events using quantification of global myocardial flow reserve in patients referred for clinical 82Rb PET perfusion imaging. J Nucl Med. 2011; 52(5):726–32. [PubMed: 21498538]
66. Ziadi MC, Dekemp RA, Williams KA, et al. Impaired myocardial flow reserve on rubidium-82 positron emission tomography imaging predicts adverse outcomes in patients assessed for myocardial ischemia. J Am Coll Cardiol. 2011; 58(7):740–8. [PubMed: 21816311]
67. Murthy VL, Naya M, Foster CR, et al. Improved cardiac risk assessment with noninvasive measures of coronary flow reserve. Circulation. 2011; 124(20):2215–24. [PubMed: 22007073]

68. Ben-Haim S, Murthy VL, Breault C, et al. Quantification of Myocardial Perfusion Reserve Using Dynamic SPECT Imaging in Humans: A Feasibility Study. J Nucl Med. 2013; 54(6):873–9. [PubMed: 23578996]
69. Slomka PJ, Berman DS, Germano G. New imaging protocols for new single photon emission CT technologies. Curr Cardiovasc Imaging Rep. 2010; 3(3):162–70. [PubMed: 20461125]
70. Wells RG, Timmins R, Klein R, et al. Dynamic SPECT Measurement of Absolute Myocardial Blood Flow in a Porcine Model. J Nucl Med. 2014 (epub ahead of print).
71. Timmins R, Klein R, Petryk J, et al. Reduced dose measurement of absolute myocardial blood flow using dynamic SPECT imaging in a porcine model. Med Phys. 2015; 42(9):5075–83. [PubMed: 26328959]
72. Nkoulou R, Fuchs TA, Pazhenkottil AP, et al. Absolute Myocardial Blood Flow and Flow Reserve Assessed by Gated SPECT with Cadmium-Zinc-Telluride Detectors Using 99mTc-Tetrofosmin: Head-to-Head Comparison with 13N-Ammonia PET. J Nucl Med. 2016; 57(12):1887–92. [PubMed: 27363834]
73. Hsu B, Chen FC, Wu TC, et al. Quantitation of myocardial blood flow and myocardial flow reserve with 99mTc-sestamibi dynamic SPECT/CT to enhance detection of coronary artery disease. European Journal of Nuclear Medicine and Molecular Imaging. 2014; 41(12):2294–306. [PubMed: 25143072]
74. Leppo JA, Meerdink DJ. Comparison of the myocardial uptake of a technetium-labeled isonitrile analogue and thallium. Circ Res. 1989; 65(3):632–9. [PubMed: 2527638]
75. Hsu B, Hu LH, Yang BH, et al. SPECT myocardial blood flow quantitation toward clinical use: a comparative study with 13N-Ammonia PET myocardial blood flow quantitation. European Journal of Nuclear Medicine and Molecular Imaging. 2017; 44(1):117–28. [PubMed: 27585576]
76. Shrestha U, Sciammarella M, Alhassen F, et al. Measurement of absolute myocardial blood flow in humans using dynamic cardiac SPECT and 99mTc-tetrofosmin: Method and validation. J Nucl Cardiol. 2017; 24(1):268–77. [PubMed: 26715603]
77. Dorbala S, Vangala D, Sampson U, Limaye A, Kwong R, Di Carli MF. Value of vasodilator left ventricular ejection fraction reserve in evaluating the magnitude of myocardium at risk and the extent of angiographic coronary artery disease: a 82Rb PET/CT study. J Nucl Med. 2007; 48(3): 349–58. [PubMed: 17332611]
78. Brodov Y, Fish M, Rubeaux M, et al. Quantitation of left ventricular ejection fraction reserve from early gated regadenoson stress Tc-99m high-efficiency SPECT. J Nucl Cardiol. 2016; 23(6):1251–61. [PubMed: 27387521]
79. Arsanjani R, Xu Y, Dey D, et al. Improved accuracy of myocardial perfusion SPECT for the detection of coronary artery disease using a support vector machine algorithm. J Nucl Med. 2013; 54(4):549–55. [PubMed: 23482666]
80. Arsanjani R, Xu Y, Dey D, et al. Improved accuracy of myocardial perfusion SPECT for detection of coronary artery disease by machine learning in a large population. J Nucl Cardiol. 2013; 20(4): 553–62. [PubMed: 23703378]
81. Arsanjani R, Dey D, Khachatryan T, et al. Prediction of revascularization after myocardial perfusion SPECT by machine learning in a large population. J Nucl Cardiol. 2015; 22(5):877–84. [PubMed: 25480110]

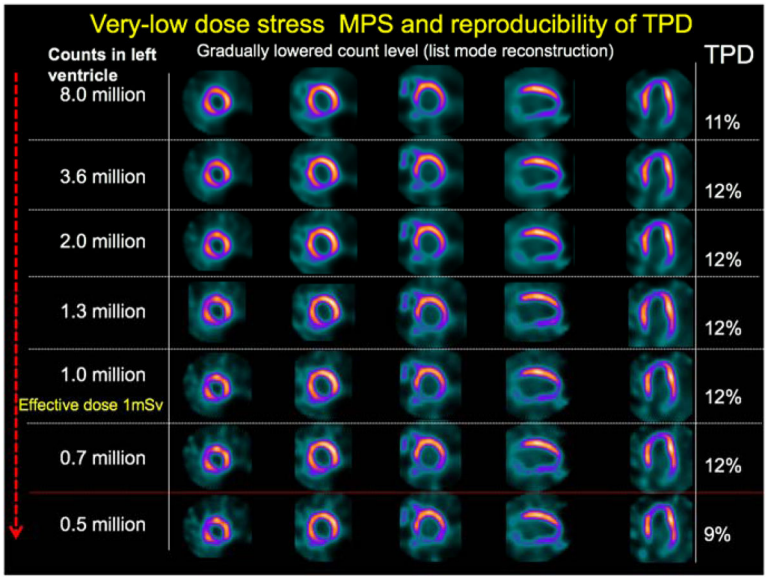

Figure 1.

Simulation of low-dose imaging. Case example of abnormal perfusion images. Total perfusion deficit (TPD) values are shown for different counts. MPS, myocardial perfusion imaging with single photon emission CT. This research was originally published in *JNM.* Nakazato et al. Myocardial perfusion imaging with a solid-state camera: simulation of a very low dose imaging protocol. *J Nucl Med.* 2013;54(3):373–9. © by the Society of Nuclear Medicine and Molecular Imaging, Inc. [3]

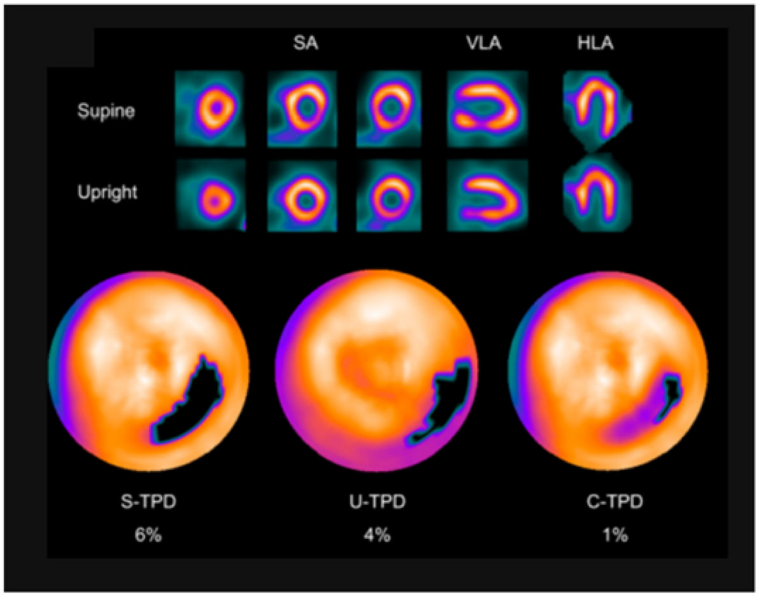

Figure 2.

Two-position imaging in Fast Myocardial Perfusion Imaging with Single Photon Emission CT (MPS). An example of inferolateral wall supine and upright MPS artifact images from a 49-y-old woman with typical chest pain and known hypertension, diabetes, hypercholesterolemia, and family history of premature CAD. The images are displayed in 3 short-axis (SA) views and in vertical long-axis (VLA) and horizontal long-axis (HLA) views. Electrocardiogram response to exercise was nonischemic for ST-segment depression. Poststress supine and upright images show reduced uptake of radiotracer in the inferolateral wall (top and middle rows). Blackout maps (bottom row) give quantification results of 4% for U-TPD and 6% for S-TPD. When supine and upright images are combined, only a small defect is visualized on black-out map, with C-TPD of 1%. The subsequent coronary angiogram showed no significant stenosis. This research was originally published in *JNM.* Nakazato et al. Quantitative upright-supine high-speed SPECT myocardial perfusion imaging for detection of coronary artery disease: correlation with invasive coronary angiography. *J Nucl Med.* 2010;51(11):1724–31. © by the Society of Nuclear Medicine and Molecular Imaging, Inc. [11]

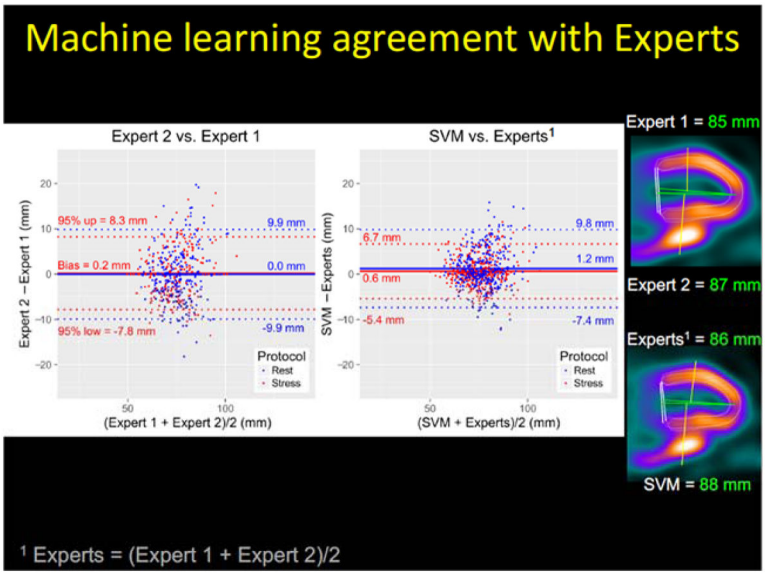

Figure 3.

Machine learning for automated valve plane position. (Left) Valve plane agreement (95% CI) between support vector machines (SVM) method and experts was lower than inter-expert agreement ($p<0.01$). Experts = (Expert 1 + Expert 2)/2. Plane position by two experts and machine learning are shown on the right. This research was originally published in *JNM*. Betancur J, Rubeaux M, Fuchs T, et al. Automatic Valve Plane Localization in Myocardial Perfusion SPECT/CT by Machine Learning: Anatomical and Clinical Validation. *J Nucl Med.* 2016 (in press) © by the Society of Nuclear Medicine and Molecular Imaging, Inc. [33].

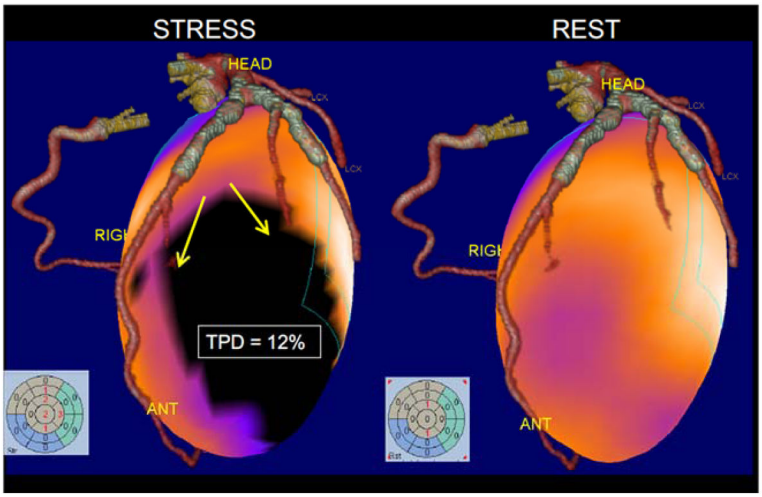

Figure 4.

Fusion of standalone CT angiography and MPS. Volume rendered 64-slice CTA fused with myocardial perfusion SPECT obtained on a different scanner at a different time. SPECT images show ischemia (3D blackout region on the left). Stress Total perfusion (TPD) was 12% in the territory supplied by the diagonal branches of LAD (as anatomically determined by CTA).

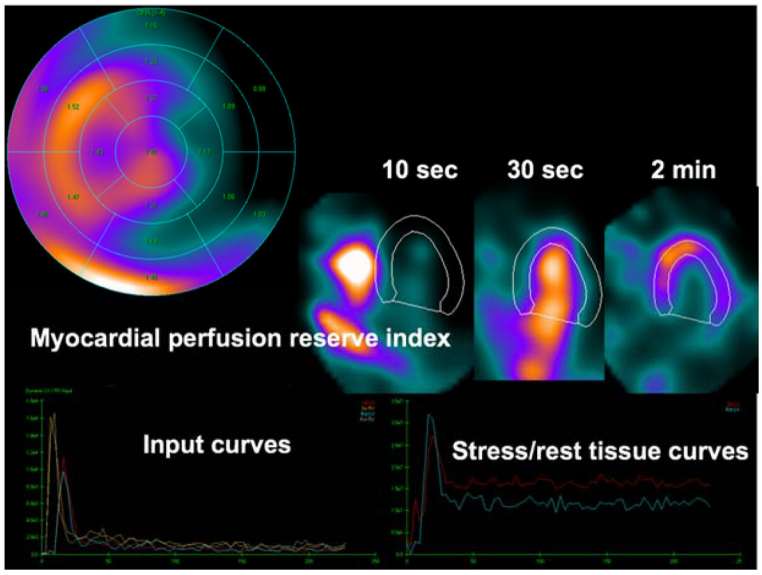

Figure 5.

Dynamic quantitative analysis of abnormal study obtained on D-SPECT system showing segmental analysis of myocardial perfusion index with segmental values (top left), dynamic images, myocardial perfusion SPECT images (top left), input curves (bottom left), and output stress and rest curves (bottom right). (Data courtesy of Marcelo Di Carli, Brigham & Women's Hospital) With kind permission of Springer: *Current Cardiovascular Imaging Reports*, New Imaging Protocols for New Single Photon Emission CT Technologies, Volume 3, 2010, pp 162–170, Slomka et al. [81].

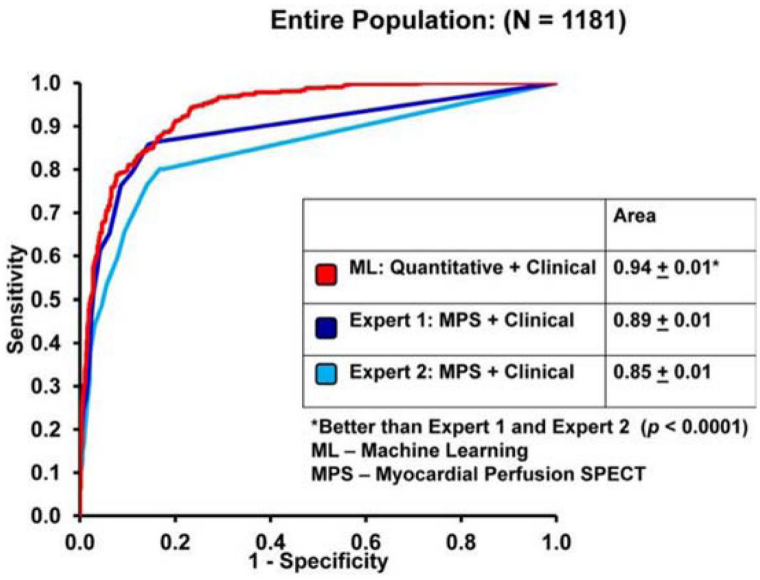

Figure 6.

Machine learning with SPECT and clinical variables. The ROC curves comparing the ML algorithm versus expert visual analysis for the detection of obstructive coronary artery disease. With kind permission of Springer: *Journal of Nuclear Cardiology,* Improved accuracy of myocardial perfusion SPECT for detection of coronary artery disease by machine learning in a large population, Volume 20, 2013, pp 553–562, Arsanjani et al. [75].